



Queensland University of Technology
Brisbane Australia

This is the author's version of a work that was submitted/accepted for publication in the following source:

Alamusi, Hu, Ning, Jia, Bi, Arai, Masahiro, Yan, Cheng, Li, Jinhua, Liu, Yaolu, Atobe, Satoshi, & Fukunaga, Hisao (2012) Prediction of thermal expansion properties of carbon nanotubes using molecular dynamics simulations. *Computational Materials Science*, 54, pp. 249-254.

This file was downloaded from: <http://eprints.qut.edu.au/75024/>

© Copyright 2011 Elsevier B.V.

NOTICE: this is the author's version of a work that was accepted for publication in *Computational Materials Science*. Changes resulting from the publishing process, such as peer review, editing, corrections, structural formatting, and other quality control mechanisms may not be reflected in this document. Changes may have been made to this work since it was submitted for publication. A definitive version was subsequently published in *Computational Materials Science*, [Volume 54, (March 2012)] DOI: 10.1016/j.commatsci.2011.10.015

Notice: *Changes introduced as a result of publishing processes such as copy-editing and formatting may not be reflected in this document. For a definitive version of this work, please refer to the published source:*

<http://dx.doi.org/10.1016/j.commatsci.2011.10.015>

Prediction of thermal expansion properties of carbon nanotubes using molecular dynamics simulations

Alamusi a, Ning Hua,b,[†], Bi Jia b, Masahiro Arai c, Cheng Yan d, Jinhua Li a, Yaolu Liu a, Satoshi Atobe e, Hisao Fukunaga e

a Department of Mechanical Engineering, Chiba University, Yayoi-cho 1-33, Inage-ku, Chiba 263-8522, Japan

b College of Metallurgy and Material Engineering, Chongqing University of Science and Technology, Chongqing 401331, People's Republic of China

c Department of Mechanical Systems Engineering, Shinshu University, 4-17-1 Wakasato, Nagano City 380-8553, Japan

d School of Engineering Systems, Queensland University of Technology, 2 George Street, G.P.O. Box 2434, Brisbane, Queensland 4001, Australia

e Department of Aerospace Engineering, Tohoku University, Aramaki-Aza-Aoba 6-6-01, Aoba-ku, Sendai 980-8579, Japan

abstract

The axial coefficients of thermal expansion (CTE) of various carbon nanotubes (CNTs), i.e., single-wall carbon nanotubes (SWCNTs), and some multi-wall carbon nanotubes (MWCNTs), were predicted using molecular dynamics (MDs) simulations. The effects of two parameters, i.e., temperature and the CNT diameter, on CTE were investigated extensively. For all SWCNTs and MWCNTs, the obtained results clearly revealed that within a wide low temperature range, their axial CTEs are negative. As the diameter of CNTs decreases, this temperature range for negative axial CTEs becomes narrow, and positive axial CTEs appear in high temperature range. It was found that the axial CTEs vary nonlinearly with the temperature, however, they decrease linearly as the CNT diameter increases. Moreover, within a wide temperature range, a set of empirical formulations was proposed for evaluating the axial CTEs of armchair and zigzag SWCNTs using the above two parameters. Finally, it was found that the absolute value of the negative axial CTE of any MWCNT is much smaller than those of its constituent SWCNTs, and the average value of the CTEs of its constituent SWCNTs. The present fundamental study is very important for understanding the thermal behaviors of CNTs in such as nanocomposite temperature sensors, or nanoelectronics devices using CNTs.

1. Introduction

Due to their superior mechanical, electrical and thermal properties, carbon nanotubes (CNTs) have many potential applications such as nanoscale sensors, nanocomposites sensors, and nanoelectronics [1–7]. For instance, for the application of nanocomposite temperature sensors [1,2] or strain sensors [6–8], it is necessary to understand the thermal properties of CNTs for developing highly efficient sensors under the different temperature environments. For some other examples of nanoelectronics including the next generation computers, e.g., [9] and nanotube transistors [10], these CNT-based nanoelectronic devices may experience high temperature during manufacture and operation. This leads to thermal expansion and residual stress in devices, and affects the device reliability. Therefore, the coefficient of thermal expansion (CTE) of CNTs is a key property for CNT-based nanoelectronics. At present, accurately evaluating CTE using experimental methods still suffers from size restrictions and measurement limitations. Therefore, computational methods, e.g., molecular dynamics (MD) simulations, prove to be an ideal tool to evaluate the CTEs. Up to date, there have been some

limited theoretical or numerical predictions on the CTE of single-wall carbon nanotubes (SWCNTs). For instance, an analytic method [11] to determine the CTE of SWCNTs directly from the inter-atomic potential and the local harmonic model was developed to evaluate the CTE of SWCNTs. Based on MD simulations, in [12,13], the CTE of SWCNTs was also studied. The influence of temperature has been mainly investigated in the above stated previous studies [11–13]. Both the axial and radial CTEs of SWCNTs have been explored. It was found that similar to Si, the axial CTE of SWCNTs displays an unusual and intriguing temperature dependence, namely being negative (i.e., thermal contraction) at low temperature, and positive (i.e., thermal expansion) at high temperature. However, due to the limitation of computational cost, only some representative SWCNTs of very small diameters have been studied, and the influence of the diameter of CNTs on the CTE of CNTs has not been studied extensively. Moreover, for the case of multi-wall carbon nanotubes (MWCNTs), the influence of the number of walls on the CTEs has not been explored to the present authors' best knowledge although MWCNTs are much more widely used in the various applications compared with SWCNTs. In this work, the CTE of CNTs was studied by using MD. We focused on the axial CTE of CNTs since the aspect ratios of CNTs are usually very high which leads to the much higher importance of the axial CTE of CNTs compared with the radial CTE of CNTs. In this paper, besides the influence of temperature on the CTE of CNTs, we also extensively explored the influence of the diameter and the number of walls of CNTs on the axial CTE.

2. MD simulations

To investigate the axial CTE of various CNTs, the direct MD simulations were carried out using the Materials Studio (Accelrys). For the case of MWCNTs, the wall spacing of any MWCNT model was given by 0.34 nm, which is close to the interlayer distance in graphite. The Lennard–Jones potential with a cut-off distance of 0.95 nm was used to describe the van der Waals (vdW) interaction among walls as used in our previous studies [14–18] and the electrostatic Coulombic interaction was also considered among walls in this study. The Universal Force Field (UFF) was employed. For modelling a single CNT, non-periodic and free-free boundary conditions were applied. The simulation process was mainly divided into the following steps:

- (1) Building up the model of CNTs of the length of 4.9 nm (see Fig. 1).
- (2) Performing the geometry optimization of CNTs using molecular mechanics (MM) to find out the initial equilibrium state.
- (3) Marking two sets of C atoms on the two sections of the distance of 2.5 nm along the CNT length direction (see Fig. 1), respectively. Note that there are 4 C atoms in one set, and this sampling distance is sufficiently long for calibrating the CTE of CNTs by referring to that the covalent C–C bond length is only around 0.14 nm. This distance was taken as the initial length (l_0) as explained later. The reason for choosing this sampling distance (2.5 nm) is from the following two aspects: (a) we calculated the CTEs by using the sampling distance ranging from 2.5–5.0 nm, and found there is no big difference; (b) when the sampling distance is much larger than 5.0 nm, the torsional deformation is significant which makes the calculation of distance change along the axial direction very difficult.
- (4) Performing the MD simulations (ensemble: NVT) with thermostats of velocity scaling at a desired temperature T , and calculating the average distance l_T between the above two

sections by using the z-coordinates of marked 8 C atoms in the two sets (see Fig. 1). Note that at one temperature, three independent computations were performed to obtain the averaged and reliable result.

(5) Calculating the axial CTE of CNTs according to the following formulation.

$$\alpha = \frac{\Delta l}{l_0} \frac{1}{\Delta T} = \frac{l_T - l_0}{l_0} \frac{1}{T - T_0} \quad (1)$$

For the MD simulations (NVT), the time step size of 0.1 fs and the total time period of 30.0 ps were taken. There were around 300,000 steps to attain the converged state for most cases. It should be noted that it is necessary to set up the initial reference temperature T_0 and its corresponding length (l_0) in the above calculation (see Eq. (1)). In this work, after the step (2) as stated above, we performed the MD simulations (NVT) at 1 K, and checked the change of average sampling distance of the above two sets of C atoms. It was found that there was almost no variation of this sampling distance, i.e., 2.5 nm. Therefore, this sampling distance, i.e., 2.5 nm, was taken as the initial length l_0 , and 0 K was approximately taken as the initial reference temperature, which was similar to that used in the most of the previous studies [11–13]. It should be noted that, for the case of MWCNTs, we also set up the above two sections along the length direction of CNTs. In this case, on each wall, there were two sets on the two sides, and each set contains 4 C atoms. Therefore, for the i th wall, we can calculate it is α_i using the similar method described for SWCNTs (see Eq. (1)), and the effective or average α for a MWCNT was simply evaluated by using the following relationship

$$\alpha = \sum_{i=1}^N \frac{\alpha_i}{N} \quad (2)$$

where N is the number of walls.

3. Results and discussions

3.1. Verification

Firstly, to verify the effectiveness of our approach for predicting the CTE of CNTs, a zigzag SWCNT(9, 0) used in some previous studies [11,13] was employed as an example. The obtained results are demonstrated in Fig. 2 compared with other two results [11,13]. From this figure, it can be found that the present result is just located between the previous two results, and possesses the similar variation trend with temperature. There is a negative CTE for the present and previous results [11,13] within the temperature of 0–500 K. When the temperature is over a certain limit (e.g., 500 K) in high temperature domain, the positive CTE appears gradually. The difference in three results may be caused by the different methods, the different sampling distances, or different potential functions or. For instance, the sampling distance l_0 in [11] was taken as 0.196 nm, which might be too short to obtain the stable and reliable CTEs if considering the C–C bond length of 0.14 nm. The influence of type of potential functions on the results seems to be very small compared with that of analysis methodologies. For instance, we also carried out the simulation based on a more complex but more accurate force field compared with UFF, i.e., COMPASS [19], which is an ab initio force field of second-generation similar to that used in the MD simulations of CTEs [20]. In Fig. 2, there is no big difference between the results of COMPASS and UFF. Moreover, in Fig. 2, the Brenner's potential [11] and the Tersoff-Brenner's potential [13] similar to

Brenner's potential were used, but their results are much different. As for analysis methods, in Ref. [11], an analytical method was employed directly based on the local harmonic model, which, however, is not of MD simulation in a real meaning. Ref. [13] employed the MD simulations (ensemble: NVE), but as shown in Fig. 2, the CTE at 0 K in [13] is not strictly zero, which disagrees with some other previous results [11,20] and the present one. This may be caused by the numerical errors in [13], or NVE ensemble used, which is unpopular in MD simulations for predicting CTE since it cannot control temperature accurately and unfortunately cannot correspond to the most common experimental conditions.

3.2. CTE of SWCNTs

After verifying the effectiveness of the present MD approach, we further investigated the influences of temperature and diameter of various large SWCNTs on CTEs since in the most of previous studies only those SWCNTs of very small diameters were explored. For various SWCNTs, the CTEs vary with temperature as shown in Fig. 3. In Fig. 3a and b, all of armchair and zigzag of SWCNTs are metallic ones. In these figures, we can identify again that the CTE varies nonlinearly with temperature. When the diameter of SWCNT is larger than 1.4 nm, i.e., for the case of zigzag SWCNT(18, 0) in Fig. 3b, there is no positive CTE in the whole temperature range from 0 K to 900 K. With the increase of the diameter of SWCNT, the CTE decreases, or its absolute value increases as shown in Fig. 3a and b. Besides the above two representative SWCNTs, the CTEs of some other SWCNTs with various chiralities (termed as chiral SWCNTs) are shown in Fig. 3c. Some SWCNTs are semi-conductive while others are metallic depending on the chiralities of SWCNTs. All of CTEs vary nonlinearly with the temperature. For both types of SWCNTs, it can be found that the CTE decreases or its absolute value increases as the diameter increases, e.g., (30, 20), (60, 40) and (80, 60) for semi-conductive SWCNTs, and (24, 18) and (48, 36) for metallic SWCNTs. The temperature range for the negative CTE becomes wider as shown in Fig. 3a–c as the diameter increases. Interestingly, compared with the semi-conductive SWCNTs, the metallic SWCNTs possess more negative CTEs from the above viewpoint of CNT's diameter. For instance, the absolute value of negative CTE of metallic SWCNT(24, 18) with the smaller diameter of 2.8 nm is higher than that of semi-conductive SWCNT(30, 20) of a larger diameter of 3.4 nm. Therefore, it can be concluded that the metallic SWCNTs are more sensitive to temperature change compared with the semi-conductive ones. At various sampling temperatures, the relationships between the CTE and the diameter of CNTs are shown in Fig. 4 for various types of SWCNTs. Fig. 4a–d shows the CTEs of armchair and zigzag SWCNTs within two temperature ranges, i.e., 1–301 K and 301–901 K, in which the CTEs behave differently as CNT's diameter changes. Fig. 4e shows the CTEs of chiral SWCNTs within 301–901 K. As shown in Fig. 4a and c, within 1–301 K, the CTEs of armchair and zigzag SWCNTs decrease linearly as the CNT's diameter increases, but with the different slopes. With the increase of temperature, they also decrease. On the other hand, within 301–901 K (see Fig. 4b and d), they decrease linearly with the diameter with the same slope. However, they increase as the temperature increases. The similar results can also be identified for chiral SWCNTs within 301–901 K as shown Fig. 4e. At 1 K, the CTE varies as a straight line of the value of 0 in all cases, which means that the reference temperature can be taken as 1 K or 0 K as described previously. At 301 K, the CTEs of all SWCNTs are close to their lowest values (also see Fig. 3). Similar to that in Fig. 3c, from Fig. 4e, we can also identify that, at the same diameter, the semi-conductive chiral SWCNTs possess comparatively smaller absolute values of negative CTEs than those of metallic chiral SWCNTs. It means that they are more insensitive to the change of temperature. By fitting the results in Fig. 4a–d, finally, within a wide temperature range (1–901 K), a set of empirical

formulations was proposed for evaluating the axial CTEs of armchair and zigzag SWCNTs using the parameters of temperature (T) and diameter (D) as follows Armchair SWCNTs:Low temperature (1–301 K)

$$\alpha = (2D - 1) \times 10^{-10}T^4 - (2D - 1) \times 10^{-7}T^3 + (2D - 5)10^{-5}T^2 - (30D - 3) \times 10^{-2}T \quad (3)$$

High temperature (301–901 K)

$$\alpha = -0.9D - (2 \times 10^{-8}T^3 - 6 \times 10^{-5}T^2 + 3 \times 10^{-2}T) \quad (4)$$

within fitting error ranging from –15% to +12% for Eqs. (3) and (4)

Zigzag SWCNTs:

Low temperature (1–301 K)

$$\alpha = -(18D + 3) \times 10^{-10}T^4 + (9D + 3) \times 10^{-7}T^3 - (D + 1)10^{-4}T^2 + (6D + 1) \times 10^{-1}T \quad (5)$$

High temperature (301–901 K)

$$\alpha = -0.4D - (2 \times 10^{-8}T^3 - 5 \times 10^{-5}T^2 + 3 \times 10^{-2}T) \quad (6)$$

within fitting error ranging from –12% to +3% for Eqs. (5) and (6) Note that D and T in the above equations are of units of nm and K, respectively. The results computed from the above empirical formulations are also illustrated in Fig. 3a and b, and in Fig. 4a–d, which are close to the results of MD. The comparison among the results of three sets of metallic armchair, metallic zigzag and metallic chiral SWCNTs is shown in Fig. 5. Note that one set of three SWCNTs is of the approximately same diameter. This figure demonstrates that, within 0–300 K, there is no obvious difference in the CTEs of the three representative SWCNTs in three sets. Beyond 300 K, except for the set of the diameter of 0.7 nm, there is no significant difference in the CTEs of the three SWCNTs in other two sets of the diameters of 2.7–2.8 nm and 5.4–5.7 nm, respectively. The CTEs of armchair SWCNTs are the highest among three results for any diameters. Moreover, the chiral SWCNTs possess the lowest CTEs, especially for the set of 0.7 nm diameter.

3.3. CTE of MWCNTs

For the case of MWCNTs, we considered two representative cases. One was a double-wall carbon nanotube (DWCNT), and the other was a triple-wall carbon nanotube (TWCNT). Firstly, an armchair SWCNT(40, 40) and a zigzag SWCNT(72, 0) were used as the innermost wall of the MWCNTs, respectively. The outer walls of different chiralities were automatically generated by Materials Studio (Accelrys) for keeping the distance between two nested walls to be 0.34 nm. For the case of the innermost wall of an armchair SWCNT(40, 40), the outermost wall for the TWCNT was SWCNT(60, 40), and the outermost wall for the DWCNT was SWCNT(60, 30), which was also the middle wall for TWCNT. For the innermost wall of a zigzag SWCNT(72, 0), the outermost wall for the TWCNT was SWCNT(90, 0), and the outermost wall for the DWCNT was SWCNT(81, 0), which was also the middle wall for TWCNT. The results of DWCNTs, TWCNTs and those SWCNTs which form the DWCNTs and TWCNTs are shown in Figs. 6 and 7, respectively. From these figures, compared to SWCNTs, we can identify that the DWCNTs and TWCNTs, which possess comparably smaller absolute values of negative CTEs, appear to be more insensitive to the change of temperature. In Fig. 6a and b, the absolute values of negative CTEs of DWCNTs are much smaller than other results of the innermost wall, the outermost

wall, and the direct average value of the above two constituent SWCNTs. The similar results can be identified for TWCNTs from Fig. 7a and b. The reason for this phenomenon is still unclear, which may be caused by the complex nonlinear coupling effects of vdW interactions among walls. The comparisons between the results of four DWCNTs and four TWCNTs are shown in Fig. 8a by referring to temperature. From this figure, we can identify that the TWCNTs possess comparatively smaller absolute values of negative CTEs than those of DWCNTs of the same innermost wall. It means that with the increase of the number of wall, the absolute value of the negative axial CTE decreases. However, compared with the differences between DWCNTs and their constituent SWCNTs, and between TWCNTs and their constituent SWCNTs in Figs. 6 and 7, the difference between TWCNTs and DWCNTs is much smaller in Fig. 8a, which implies that the CTEs gradually saturate when the number of wall is over 3. Moreover, in Fig. 8a, for those MWCNTs of small diameters, e.g., T(20, 20) and D(20, 20), there are positive CTEs in high temperature range. It was also found that the CTEs of DWCNTs and TWCNTs do not vary linearly with temperature (see Fig. 8a). Within 301–901 K, Fig. 8b shows that the CTEs of three DWCNTs and three TWCNTs, which are of (20, 20), (40, 40) and (60, 60) as innermost walls, respectively, vary linearly with the diameter of the innermost wall at five typical temperatures. With the increase of the diameter, the axial CTEs of DWCNTs and TWCNTs decrease. Moreover, at the same diameter of the innermost wall, the CTEs of DWCNTs is a slightly lower than those of TWCNTs. Fig. 8c shows the CTEs of a DWCNT, a TWCNT, CNTs of four, five and six walls. It can be found that the CTE curve move up gradually with the increase of the number of walls. However, the converged CTE can be identified for the CNT of five walls, which confirms our previous speculation.

4. Summary

In this work, we investigated the axial CTEs of various CNTs, e.g., SWCNTs and MWCNTs, by using MD simulations. It was found that the axial CTEs of CNTs are negative in a wide low temperature range, and vary nonlinearly with the temperature. These axial CTEs may become positive as the temperature increases, especially for those SWCNTs and MWCNTs of small diameters of the innermost wall. However, the axial CTEs of SWCNTs and MWCNTs vary linearly with the diameter of the innermost wall. With the increase of the diameter, the axial CTEs decrease. For the case of SWCNTs, compared to metallic chiral SWCNTs, the semi-conductive chiral SWCNTs, which possess comparatively smaller absolute values of negative CTEs, appear to be more insensitive to the change of temperature. Within a wide temperature range, a set of empirical formulations was proposed for evaluating the axial CTEs of the armchair and zigzag SWCNTs using the temperature and the CNT's diameter. For MWCNTs, their CTEs cannot be simply evaluated from the average CTE of their constituent SWCNTs forming the MWCNTs. Generally, with the increase of the number of wall, within the low temperature range, the absolute values of negative CTEs of MWCNTs become smaller gradually within low temperature range, and finally converge to a stable value when the number of wall is 5. This indicates that the MWCNTs become more insensitive to the change of temperature as the number of wall increases.

Acknowledgements

This work is partly supported by two Grand-in-Aids for Scientific Research (Nos. 22360044 and 21226004) from the Japanese Ministry of Education, Culture, Sports, Science and Technology. The authors acknowledge Prof. C.B. Fan (Beijing Institute of Technology, China) for kindly providing the computational resources.

References

- [1] A. Saraiya, D. Porwal, A.N. Bajpai, N.K. Tripathi, K. Ram, *Met.-Org. Nano-Met. Chem.* 36 (2006) 163.
- [2] H.C. Neitzert, A. Sorrentino and L. Vertuccio, Epoxy/MWCNT Composite Based Temperature Sensor with Linear Characteristics, in: P. Malcovati, et al., (Eds.) *Sensors and Microsystems. AISEM 2009 Proceedings, Lecture Notes in Electrical Engineering*, vol. 54, Part 3, 2010, pp. 241.
- [3] R.S. Ruoff, D.C. Lorents, *Carbon* 33 (1995) 925.
- [4] D. Srivastava, M. Menon, K.J. Cho, *Comput. Sci. Eng.* 3 (2001) 42.
- [5] B.I. Yakobson, P. Avouris, *Topics of Applied Physics* in: M.S. Dresselhaus, G. Dresselhaus, P. Avouris, (Eds.), *Carbon Nanotubes*, vol. 80, 2001, pp. 287.
- [6] N. Hu, Y. Karube, Y. Cheng, Z. Masuda, H. Fukunaga, *Acta Mater.* 56 (2008) 2929.
- [7] N. Hu, Y. Karube, M. Arai, T. Watanabe, C. Yan, Y. Li, Y. Liu, H. Fukunaga, *Carbon* 48 (2010) 680.
- [8] G. Yin, N. Hu, Y. Karube, Y. Liu, Y. Li, H. Fukunaga, *J. Compos. Mater.* 45 (2011) 1315.
- [9] J.R. Heath, *Pure Appl. Chem.* 72 (2002) 11.
- [10] S.J. Tans, A.R.M. Verschueren, C. Dekker, *Nature (London)* 393 (1998) 49.
- [11] H. Jiang, B. Liu, Y. Huang, K.C. Hwang, *J. Eng. Mater. Tech.* 126 (2004) 265.
- [12] N.R. Raravikar, P. Keblinski, A.M. Rao, M.S. Dresselhaus, L.S. Schadler, P.M. Ajayan, *Phys. Rev. B* 66 (2002) 235424.
- [13] M.N. Prakash, Determination of coefficient of thermal expansion of singlewalled carbon nanotubes using molecular dynamics simulations. PhD. Thesis, The Florida State University, 2005.
- [14] N. Hu, H. Fukunaga, C. Lu, M. Kameyama, B. Yan, *Proc. Royal Soc. A* 461 (2005) 1685.
- [15] N. Hu, K. Nunoya, D. Pan, T. Okabe, H. Fukunaga, *Int. J. Solids Struct.* 44 (2007) 6535.
- [16] Y. Li, N. Hu, G. Yamamoto, Z. Wang, T. Hashida, H. Asanuma, C. Dong, T. Okabe, M. Arai, H. Fukunaga, *Carbon* 48 (2010) 2934.
- [17] Y. Li, Y. Liu, X. Peng, Y. Cheng, S. Liu, N. Hu, *Comput. Mater. Sci.* 50 (2011) 1854.
- [18] S. Liu, N. Hu, G. Yamamoto, Y. Cai, Y. Zhang, Y. Liu, Y. Li, T. Hashida, H. Fukunaga, *Carbon* 49 (2011) 3698.
- [19] M.G. Martin, *Fluid Phase Equilibr.* 248 (2006) 50.
- [20] Y. Kwon, S. Berber, D. Tomanek, *Phy. Rev. Lett.* 92 (2004) 015901.

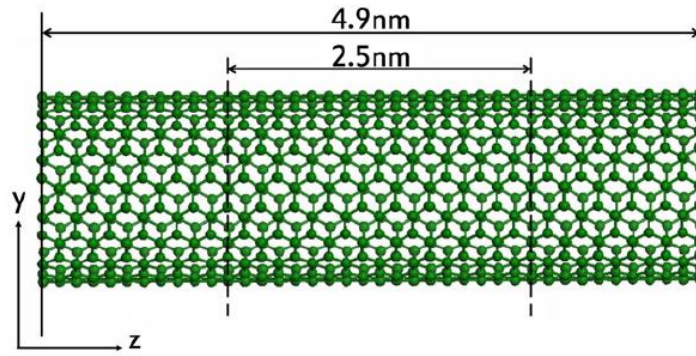


Fig. 1. Schematic view of a SWCNT model and sampling distance for evaluating CTE.

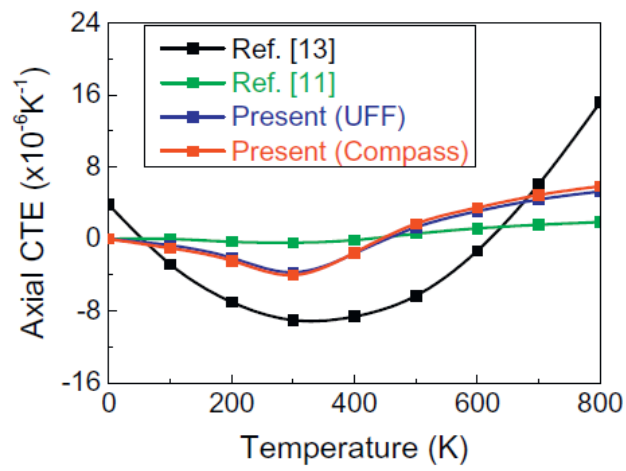


Fig. 2. Comparison of various CTEs for a zigzag SWCNT(9, 0).

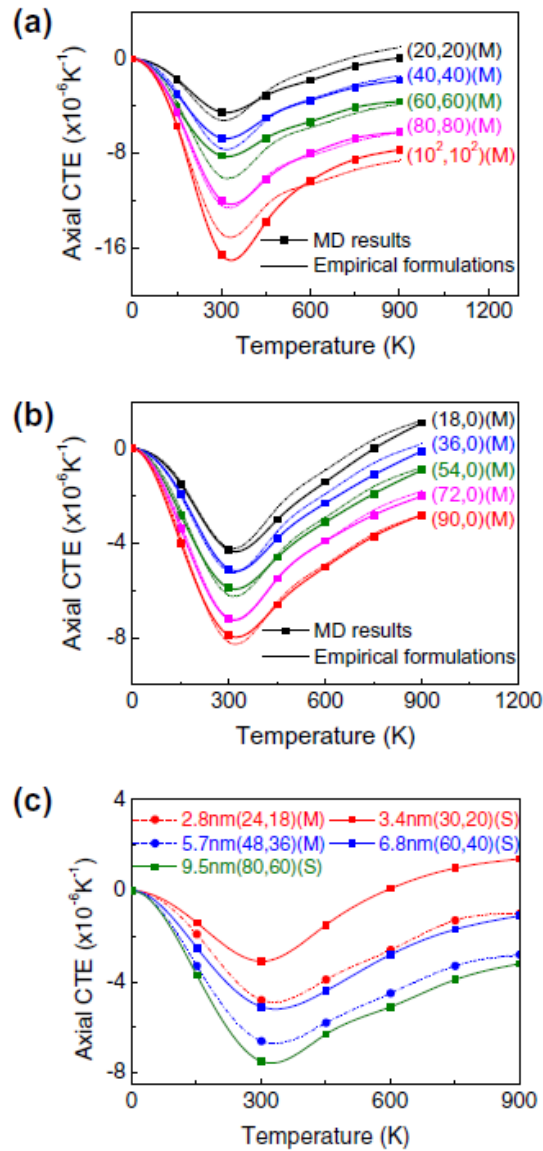


Fig. 3. Influence of temperature on CTEs of armchair, zigzag and chiral SWCNTs. (a) Armchair SWCNTs (the integers in brackets (n, m) are chirality indices of CNTs. The diameter of CNTs increases from 2.7 nm for $(20, 20)$ to 13.5 nm for $(100, 100)$ with 2.7 nm increment. The symbol of "M" is for metallic CNTs). (b) Zigzag SWCNTs (the integers in brackets (n, m) are chirality indices of CNTs. The diameter of CNTs increases from 1.4 nm for $(18, 0)$ to 7.0 nm for $(90, 0)$ with 1.4 nm increment. The symbol of "M" is for metallic CNTs). (c) Chiral SWCNTs (the figures after the line symbol is the diameter of CNTs, the integers in brackets (n, m) are chirality indices of CNTs, the symbol of "S" is for semi-conductive chiral SWCNTs, and "M" is for metallic chiral SWCNTs).

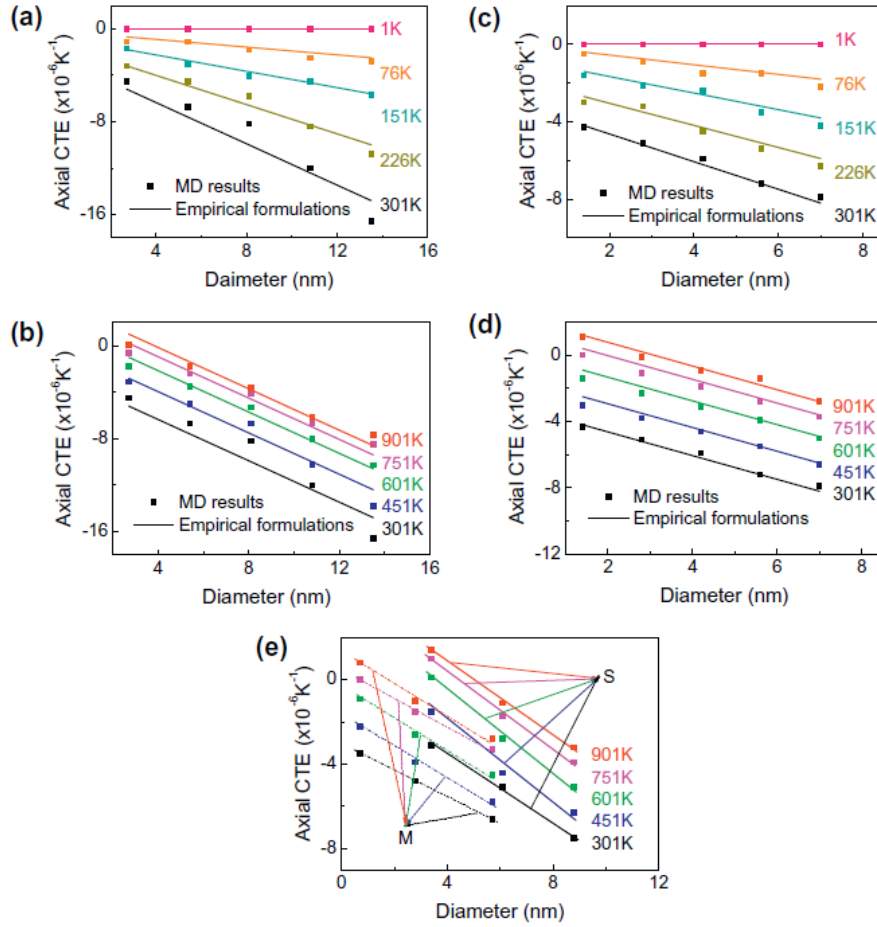


Fig. 4. Influence of diameter on CTEs of armchair, zigzag and chiral SWCNTs. (a) Armchair SWCNTs (1–301 K). (b) Armchair SWCNTs (301–901 K). (c) Zigzag SWCNTs (1–301 K). (d) Zigzag SWCNTs (301–901 K). (e) Chiral SWCNTs (301–901 K) (the symbol of "M" is for metallic SWCNTs, and "S" is for semi-conductive SWCNTs).

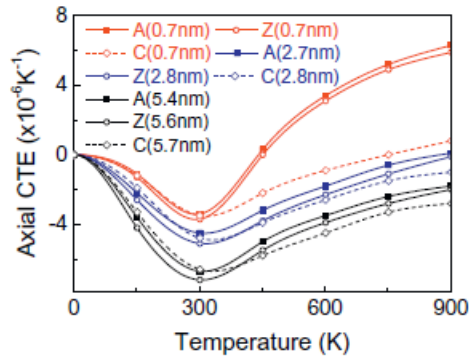


Fig. 5. Comparison of CTEs of armchair, zigzag and chiral SWCNTs (the symbol of "A" is for armchair SWCNTs, the "Z" is for zigzag SWCNTs, and the "C" is for chiral SWCNTs, the figures in front of "(M)" are CNT's diameters, and the symbol of "M" is for metallic SWCNTs).

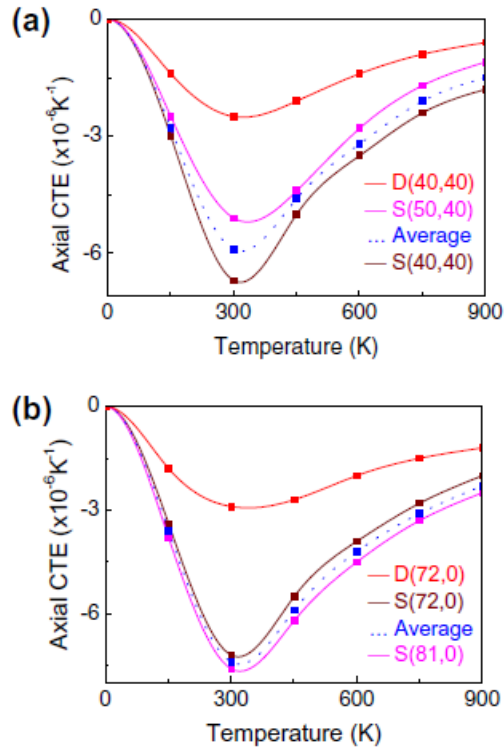


Fig. 6. CTEs of two DWCNTs and their constituent SWCNTs. (a) A DWCNT(40, 40) (two constituent SWCNTs are inner wall of SWCNT(40, 40) and outer wall of SWCNT(50, 40), the symbol of "D" is for the DWCNT, and "S" is for the SWCNTs, and "Average" is average value of CTEs of two SWCNTs). (b) A DWCNT(72, 0) (two constituent SWCNTs are inner wall of SWCNT(72, 0) and outer wall of SWCNT(81, 0), the symbol of "D" is for the DWCNT, and "S" is for the SWCNTs, and "Average" is average value of CTEs of two SWCNTs).

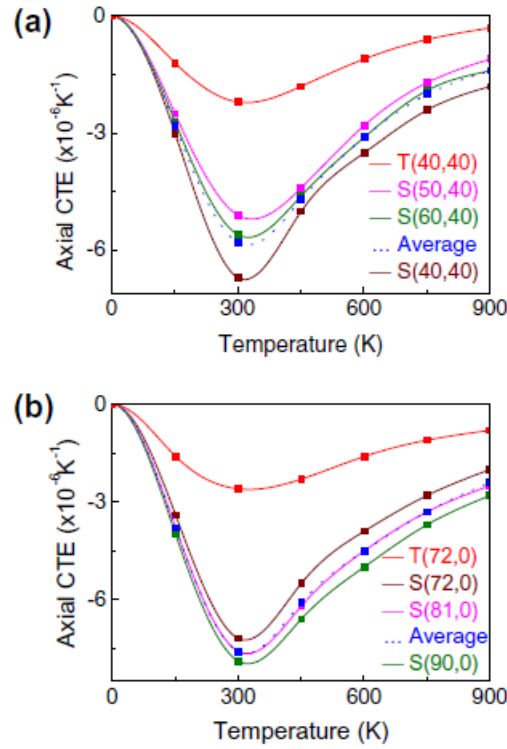


Fig. 7. CTEs of two TWCNTs and their constituent SWCNTs. (a) A TWCNT(40, 40) (three constituent SWCNTs are innermost wall of SWCNT(40, 40), middle wall of SWCNT(50, 40) and outermost wall of SWCNT(60, 40), the symbol of "T" is for the TWCNT, and "S" is for the SWCNTs, and "Average" is average value of CTEs of three SWCNTs). (b) A TWCNT(72, 0) (three constituent SWCNTs are innermost wall of SWCNT(72, 0), middle wall of SWCNT(81, 0) and outermost wall of SWCNT(90, 0), the symbol of "T" is for the TWCNT, and "S" is for the SWCNTs, and "Average" is average value of CTEs of three SWCNTs).

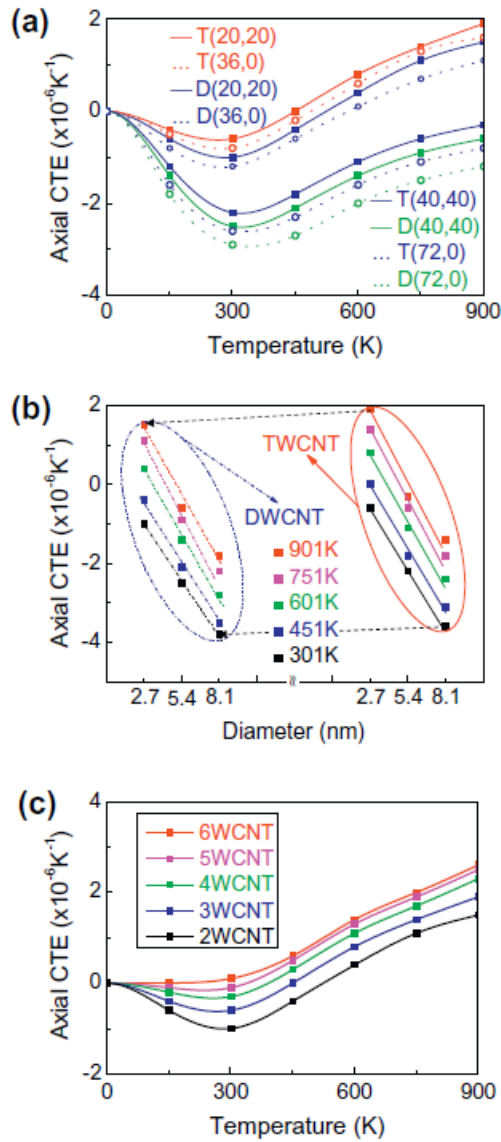


Fig. 8. Comparison of CTEs of MWCNTs. (a) CTEs of DWCNTs and TWCNTs versus temperature (the symbol of "T" is for the TWCNT, the symbol of "D" is for the DWCNT, and the integers in brackets (n, m) are chirality indices of the innermost wall). (b) CTEs of DWCNTs and TWCNTs versus diameter of innermost wall. (c) CTEs of MWCNTs versus temperature (innermost wall is SWCNT (20, 20) for all cases).